

Title	Nonlinear Dynamics of a Collective Optical Element
Author(s)	Otsuka, Kenju; Ikeda, Kensuke
Citation	物性研究 (1987), 48(4): 326-333
Issue Date	1987-07-20
URL	<a href="http://hdl.handle.net/2433/92622">http://hdl.handle.net/2433/92622</a>
Right	
Type	Departmental Bulletin Paper
Textversion	publisher

神経線維の周期刺激応答に見られるChaos

慶大・理工 羽生 義郎

東工大・統理工 高橋 信行

電総研 松本 元

生理的環境下にあるヤリイカ巨大軸索に周期刺激を与えた時の膜電位応答を調べた。刺激の周期と大きさを bifurcation parameter として応答の two dimensional bifurcation diagram を得た。(図1) 刺激の強さ(周期・大きさ)がある臨界値より大きい時は、応答は周期的であり、その時、発火率は bifurcation parameter に対して単調な階段状の関数となるが、小さい時は、非周期的な応答が存在し、そこでは発火率が減少していた。その非周期的応答が、chaos である事を correlation integral の方法から確めた。(図2に chaotic response の一例を示す。) chaos への bifurcation は、一方は subcritical period-doubling に続く intermittency, もう一方は crisis である事がわかった。又、周期刺激により発生した chaotic response が軸索上を安定に伝播する事を見出した。

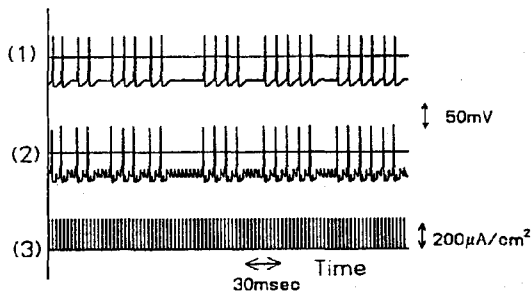


図1 Schematic Diagram showing dependence of Firing Rate & Patterns upon  $I/I_t$  and Pulse Interval ( 1 : firing, 0 : nonfiring )

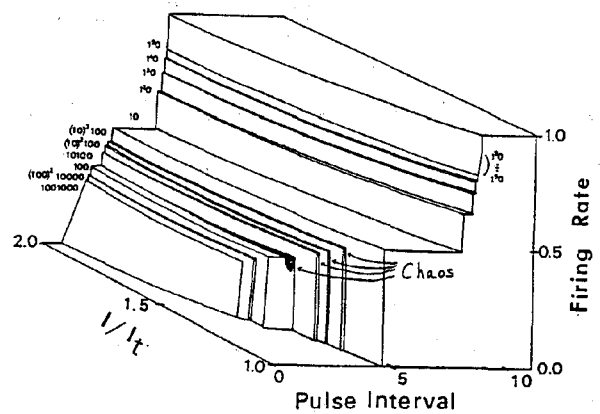


図2 Chaotic Responses  
 (1) stimulation current pulses  
 (2) non-propagated responses  
 (3) propagated responses

Nonlinear Dynamics of a Collective Optical Element

Kenju Otsuka NTT Electrical Communications Laboratories, Musashino-shi, Tokyo 180

Kensuke Ikeda Research Institute for Fundamental Physics, Kyoto University, Kyoto 606

§1 Introduction

It has recently been recognized that many temporally irregular phenomena consist of nothing

more than the intrinsic chaos inherent in the rules of their evolutionary processes. The question then arises as to whether it is possible to understand spatially irregular structures in terms of the intrinsic chaos inherent in the rule which determines their spatial arrangements? In equilibrium systems, the spatial chaos derived from the rule of spatial arrangement is unlikely to be a true ground state and is more probably a thermodynamically metastable state.<sup>1</sup> The possibility of the existence of spatial disorder has been predicted in a nonlinear optical system, which is a typical example of macroscopic nonequilibrium physical systems.<sup>2</sup> However, the dynamical stability of such spatial disorders, which is the essential problem, is not clearly understood. In §2, we present a simple dynamical system consisting of distributed nonlinear optical media and show that spatial disorder exists quite stably over a wide range of the control parameter.

On the other hand, collective behavior, which arises through the interaction of elemental components, is expected to be qualitatively different from the sum of the individual parts. In §3, an interesting collective behavior in the proposed system featuring domino dynamics, cooperative switching, assignment of bifurcate spatial patterns as well as multivibrator operations, is also shown to be reliable in light of practical application.

## §2 Frozen spatial disorder

The conceptual model is shown in Fig. 1. In the model, nonlinear elements possessing third-order susceptibility are arranged in a looped optical ring cavity. These elements interact via counterpropagating light beams that are introduced through the mirrors which separate the elements. Within the limit of large dissipation ( $B \ll 1$ ) and  $A^2 B \sim 0(1)$ , the dynamics are governed by<sup>3</sup>

$$\tau \dot{\phi}_k = -\phi_k + f_F(\phi_{k-1}) + f_B(\phi_{k+1}), \quad \phi_{N+1} = \phi_1, \quad f_{F,B}(\phi) = A_{F,B}^2 [1 + 2B \cos(\phi + \phi_0)], \quad k=1, 2, \dots, N \quad (1)$$

where  $\phi_k$  is the phase shift introduced into the field when the field passes across the  $k$ -th element,  $\phi_0$  is the linear phase shift, and  $B = \sqrt{T}$  is the coupling coefficient between adjacent cells. The nonlinear grating effect as well as the medium loss are neglected and  $\tau/(L/c) \gg 1$  ( $\tau$ : response time,  $L$ : cell length,  $c$ : velocity of light) is assumed.

First let us consider the case of unidirectional interaction, i.e.  $A_F = A$  and  $A_B = 0$ . In this case, the stationary solution,  $\phi_k$ , of Eq. (1) is determined by the mapping rule  $\bar{\phi}_{k+1} = f_F(\bar{\phi}_k)$ , with  $\bar{\phi}_{N+1} = \bar{\phi}_1$ . The bifurcation diagram for  $\phi_0 = 0$  is depicted in Fig. 2. These solutions are easily found to be "chaotic" if  $2A^2B$  is made sufficiently large. The most important point in

our problem is the dynamical stability of  $\bar{\phi}_k$ . From a linear stability analysis, the spatial structure is shown to be dynamical stable if  $\phi_k$  is the stable solution of the map, that is  $\alpha = (1/N) \sum_{k=1}^N \ln |f_F'(\bar{\phi}_k)| < 0$  in the limit of  $N \rightarrow \infty$ , where  $\alpha$  is the "spatial" Lyapunov exponent. In general, when  $q$  is a divisor of  $N$ , period  $q$ -cyclespatial patterns can be stabilized. In the case of  $N = 2^n$  ( $n$ :integer), in particular, a spatial period-doubling bifurcation takes place and period-doubled structures are frozen stably. Stable solutions for  $N = 2^n \cdot p$  ( $p \forall$  integer  $\neq 1, 2$ ) can be classified into two classes. One implies a period 1-cycle solution and  $1 \times 2^n$  solutions period-doubled from the period-1 solution ( $S(1)$ ). The other consists of period- $N$  and  $-p$  cycle solutions originating from tangential bifurcation and  $p \times 2^n$ -cycle solutions period-doubled from the period  $p$ -cycle solution  $S(p)$ . The result for  $N = 2^1 \times 3$  is shown in Fig.3. Period-doubled solution is frozen stably (See (b)).<sup>5</sup> Is the  $S(p)$  structure realized as  $A$  increases up to the stable domain of  $S(p)$ ? This is not the case and dynamical instability, which leads to spatiotemporal chaos (STC) when  $N \gg 1$ , develops instead. This is due to the fact that  $S(p)$  solutions, including the unstable regions, form closed loops (isolas) and these are isolated from  $S(1)$ . In addition, their stable regions localize at the edges of the isolas (See Fig.3(a)). As  $p$  increases, stable regions of  $S(p)$  decrease and the basin of attraction of  $S(p)$  decreases exponentially, becoming narrower than that of STC. As a result, STC's which connect to  $S(1)$  are realized and the  $S(p)$  structures are not frozen (Fig.3(b)).

Next let us consider the case of bidirectional interaction. In this case, the dynamics are dramatically changed. Even if  $r = A_B^2/A_F^2$ , which represents the symmetry of the system ( $\leq 1$ ) is equal to unity, Eq. (1) lacks the potential condition of  $\partial \dot{\phi}_k / \partial \phi_{k-1} = \partial \dot{\phi}_{k-1} / \partial \phi_k$  and thus there is no Lyapunov functional which corresponds to a Hamiltonian (or free energy) in equilibrium systems. This fact does not ensure an approach to static structures. Indeed, in the high intensity regime, STC is developed. However, in the low intensity regime, period  $N$ -cycle spatial solutions are found to be frozen over a wide region!  $\phi_k$  are plotted, except for transients, as  $P = A_F^2 + A_B^2$  is increased (decreased) very slowly in the case of  $r = 1$  (Fig.4(b)).  $\phi_k$  varies stepwise with  $P$ , being accompanied by hysteresis, and on the lower intensity side of each step,  $\phi_k$  is bi(multi)-furcated into  $N$  different static values. Moreover, the global structure does not depend on the system size. It is difficult to judge rigorously whether such a structure is really the "ground state" or not however, it does not collapse even under the presence of noise. An example of disordered structures and the corresponding "spatial" return map are shown in Fig.5. Fig.5(a) features an almost period 2-cycle structure with "holes" in it. Such holes result from homoclinic orbits originating from a period 2 fix point as is seen in Fig.4(b). The stabilization mechanism of such structures is currently under study.

### §3 Collective behavior

In this section, we examine the cooperative behavior in the case of unidirectional interaction. Assume that  $N \gg 1$  and the system is set on the upper state  $\phi_u$  of "S"-shaped bistable region, where  $A_k^2 (k=1, 2, \dots, N) = 11$ ,  $B = 0.1$  and linear phase shift of  $\phi_0 = 0$ . Here, we apply an excitation pulse of  $A_p^2$  only to one cell  $k=1$ . Then,  $\phi_1$  tends to relax to a new state  $\phi_1' = f(\phi_u) \equiv A_1'^2 g(\phi_u)$  ( $A_1'^2 = A_1^2 + A_p^2$ ) roughly within a  $\tau$  period. When  $\phi_1'$  is realized, then the states of following cells are successively determined like "domino theory" based on the mapping rule of  $\phi_k' = A_k^2 g(\phi_{k-1}')$ ,  $k = 2, 3, \dots, N$ . The dynamics differ depending upon  $A_p^2$ , and can be classified as follows:

(1) all  $\phi_k$  remain in the upper branch, (2) all  $\phi_k$  switch down to the lower branch, (3) all  $\phi_k$  exhibit up-down pulsation at every round trip (astable multivibration), where (1) is realized in regions A, D, (2) is realized in region B, and (3) takes place in region C in Fig.6(a). On the other hand, when all cells are initially set on the lower state  $\phi_l$ , dynamics can also be classified into the following three categories: (1) all  $\phi_k$  remain in the lower branch in regions A and B, (2) all  $\phi_k$  exhibit astable multivibration in region C, and (3) all  $\phi_k$  switch up to the upper branch in region D. In order to confirm the above dynamics, numerical simulations are carried out using Eq. (1), where  $N = 6$ ,  $A_k^2 = 11$ ,  $B = 0.1$  and  $\phi_0 = 0$  are assumed. Results for the former case are depicted in Fig.6(b). These results clearly reproduce the analytical predictions. It should be noted that  $\phi_k$  relaxes to stable fixed points and period 6-cycle spatial structures are realized stably in region A, B and D. This indicates that the input information on the  $k = 1$  cell is converted into different spatial patterns. In fact,  $N$ -length  $2^N$  binary inputs determined by the arrangement of  $\{A_p(\alpha)\}$  ( $k=1, 2, \dots, N$ ) are found to be converted into the same number of spatial patterns for  $N = \text{prime number}$ .

Next let us consider the assignment of the system to bifurcated structures in the hysteretic regime. This is realized by "modulating" the map. In short, one applies an excitation pulse  $A_p^2$  such that the  $\phi_1$  tends to relax to one of  $\{\bar{\phi}_k\}$  of the period  $q$ -cycle solution and then cuts off the pulse at the time when such a solution has been established. Hereupon, states of the following cells successively relax to the desired  $q$ -cycle solutions. The result of this assignment to the period 4-cycle solution, shown in Fig.7, indicates that the input can be stored as spatial patterns.

Finally, let us consider bistable multivibrator operation which provides key functions for various types of logic. Such operations can be achieved by applying optical pulses (trigger) with finite pulsewidth to a single cell. It is easy to find that  $A_p^2$  of trigger pulse should be set within regions B or C to realize an off-switch and in regions C or D to realize an on switch. In order

to achieve multivibrator operation, however, the pulsewidth must be chosen in the proper regions. The timing for cutting off the trigger pulse is determined such that the greater portion of  $\phi_k$  has already crossed over the saddle at the trailing edge of the trigger pulses. Such a "majority" condition can be understood in terms of the "domino" mechanism. Numerical results are depicted in Fig.8 for  $N = 6$ . The present scheme provides various flip-flop functions, such as T(Toggle), SR(Set-Reset) and D(Delay).<sup>6</sup> A variety of spatial structures discussed in bidirectional interaction might serve as the basis for novel optical memory device which stores complicated input information as spatial patterns. Indeed, bistable multivibration operations featuring  $N$ -cycle spatial patterns are proved to be realizable when  $N$  is not so large.

#### §4 Conclusion

The stabilization of spatial disorder has been predicted for the first time in a macroscopic nonequilibrium system (nonlinear optical system). The study of the relationship between spatio-temporal chaos and the large number of coexisting frozen random patterns may provide an important clue for understanding turbulence phenomena.

Novel cooperative behavior based upon "domino"-like dynamics has also been theoretically demonstrated on all optical basis. We expect that the proposed device will be of considerable interest in the field of optical computing.

One of the authors (K.O) is very grateful to Dr. T. Kimura for his encouragement.

#### References

1. S. Aubry, in Solitons and Condensed Matter Physics, ed. by A. R. Bishop and T. Schneider (Springer-Verlag, Berlin 1979) p.264.
2. J. Yumoto and K. Otsuka, Phys. Rev. Lett. 54, 1806 (1985).
3. K. Ikeda and M. Mizuno, IEEE J. Quantum Electron. QE-21, 1429 (1985).
4. If  $\sigma = \prod_{k=1}^N f_F'(\bar{\phi}_k) < 0$  (inverted bifurcation),  $\phi_k$  is dynamically stabilized in the region of  $0 < \alpha < \ln|1/\cos(\pi/N)|$ . However, this region becomes negligibly small compared with that for  $\alpha < 0$  in the limit of  $N \gg 1$ .
5. As  $A$  increases into the period-4 cycle region, which does not exist in the steady-state for  $N = 6$ , the  $\phi_k$  of every other cell tends to wander between the upper and lower branch bifurcated from each period-2 cycle solution at every round trip (See Fig. 3 (b)).
6. K. Otsuka and K. Ikeda, Optics Lett. (1987), in press.

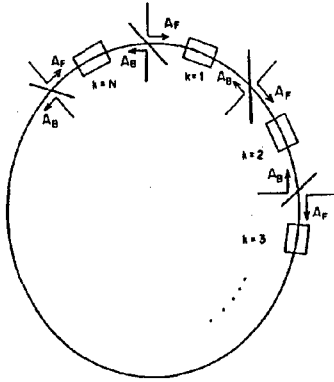


Fig.1 Conceptual model of an optical bistable system with distributed nonlinear media.

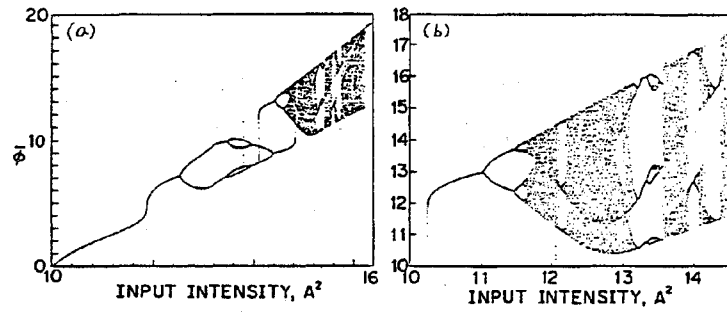


Fig.2 Bifurcation diagram for  $B = 0.1$ ,  $\phi_0 = 0$ . (b) is the enlargement in the region  $A^2 > 10$ .

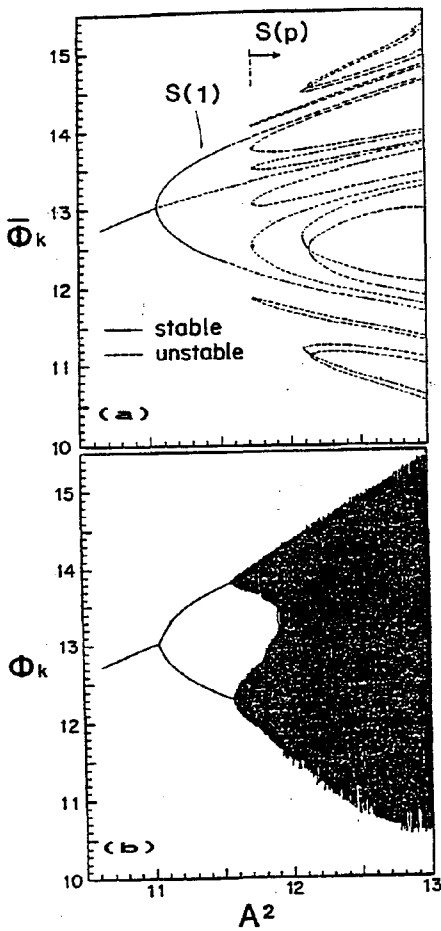


Fig. 3

Fig.3 (a) Spatial bifurcation diagram  $B = 0.1$ ,  $\phi_0 = 0$ , and  $N = 2^1 \times 3$ .

Solid curves and dotted curves respectively correspond to stable and unstable solutions.

(b)  $\phi_k (k=1, 2, \dots, N)$  versus  $A^2$  for  $N = 2^1 \times 3$

Fig.4  $\phi_k (k=1, 2, \dots, N)$  versus  $P$ .  $B = 0.3$ ,  $\phi_0 = 0$ ,  $N = 23$ .

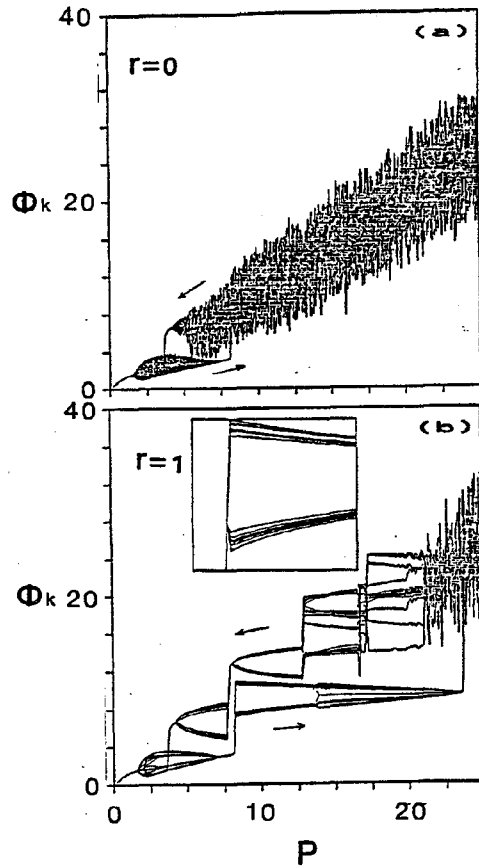


Fig. 4

(a)  $r = 0$  (unidirectional) (b)  $r = 1$  (bidirectional) The insert in (b) depicts the enlargement around  $P = 10$ . In this case, symmetric period  $N$  solutions are realized and bifurcation into 12 different states is seen. Period  $N$ -cycle nonsymmetrical solutions can also be realized by asymmetrical excitation, i. e.  $r \neq 0, 1$

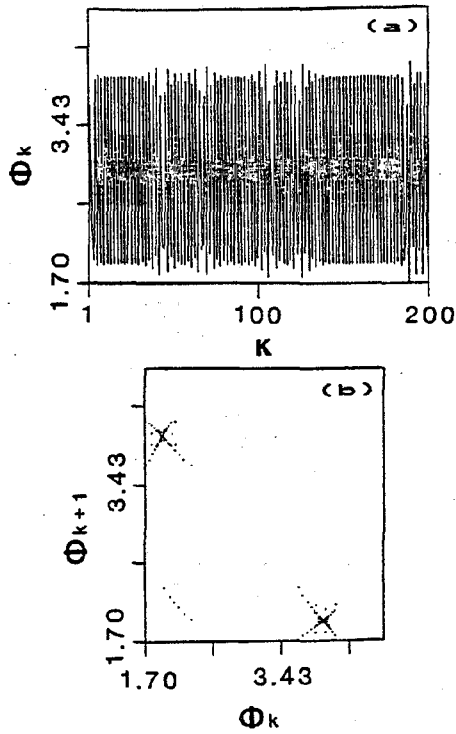


Fig. 5

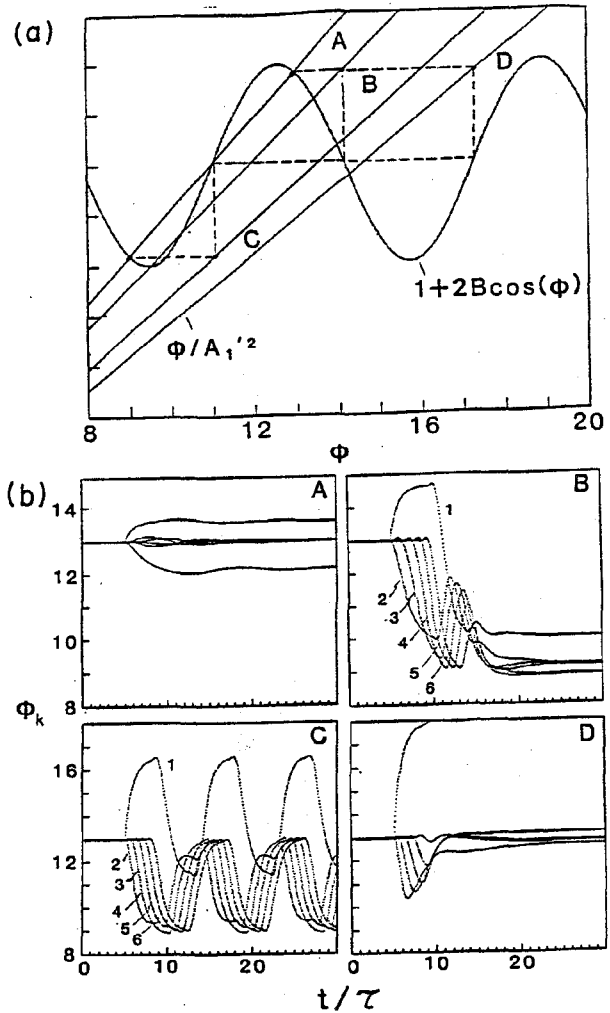


Fig. 6

Fig.5 An example of frozen disordered patterns which is self-induced by increasing  $P$  to 6, where  $N = 200$  and  $r = 1$ . (a) Self-induced spatial disorder (b) Spatial return map.

Fig.6 Relaxation dynamics when one cell ( $k = 1$ ) is excited.  $N = 6$ ,  $B = 0.1$  and  $\phi_0 = 0$ .

A:  $A_p^2 = 0.5$ , B: 1.4, C: 3.0, D: 4.2



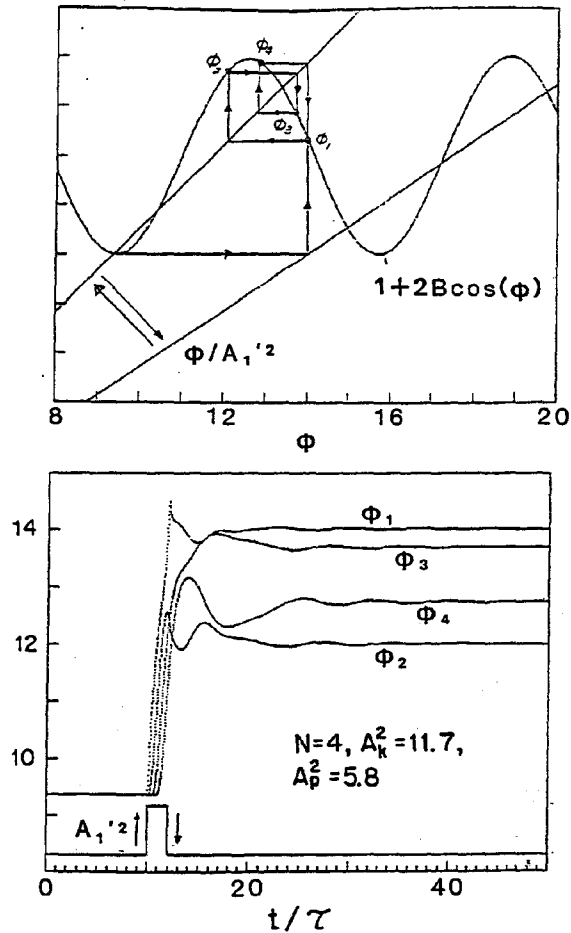


Fig. 7

Fig.7 Assinment to period 4-cycle solution.  $N = 4, A_k^2 = 11.7, A_p^2 = 5.8$

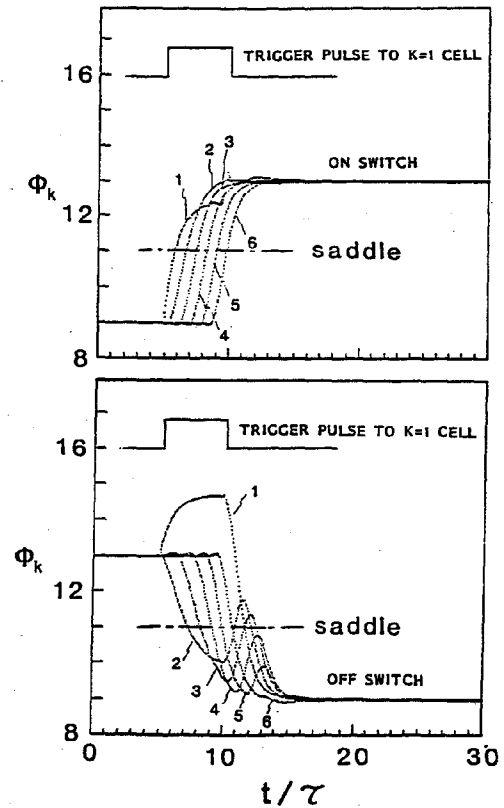


Fig. 8

Fig.8 Cooperative bistable multivibrator operation.  $N = 6, A_k^2 = 11, A_p^2 = 3$

## 多モードレーザーからのカオス光とその統計的性質

東大・工 小川 哲 生

### 1. 序 論

時間的インコヒーレント光を用いるレーザー分光法の発展<sup>1)</sup>に伴い、用いられるレーザー光の統計的性質を明らかにすることが必要となっている。多モードレーザーから発生する良く制御された光カオスは、その光源として有力な候補の一つである。さらに、多モードレーザー系の発振過程の解析から、動特性、変調特性を明らかにし、Lorenzカオスやそのパラメータ変調効果を解明することは、非平衡非線型開放系の研究としても大きな価値がある。そこで、反転